# Active Region Emissions and Coronal Field Extrapolations

Jeongwoo Lee
*Physics Department, New Jersey Institute of Technology, Newark, NJ 07102, U.S.A.*
*E-mail: leejw@njit.edu*

Stephen M. White, Mukul R. Kundu
*Astronomy Department, University of Maryland, College Park, MD 20742, U.S.A.*

Zoran Mikić
*Science Applications International Corporation, San Diego, CA 92121, U.S.A.*

**Abstract**

With vector magnetographs set to fly on the Solar–B mission, the extrapolation of photospheric magnetic fields into the corona will be increasingly important. As the techniques of coronal field extrapolations grow more sophisticated, we require a more powerful means to test them and to make full use of the information they contain. Radio data can play an important role in testing extrapolation methods. In this paper, we discuss a new test of coronal field extrapolation using the concept of *field line connectivity*. The motivating idea is that temperature should be nearly uniform on a given magnetic field line due to the rapid transport of physical quantities along field lines in the corona. Optically–thick gyroresonance emission provides the temperature on a surface of known magnetic field strength in the corona. As a consequence, we may expect that radio intensities observed at different frequencies at points connected by field lines should show a good correlation. This suggests that a test of a magnetic field extrapolation model is whether the field–line connectivity it predicts shows such a correlation. A second application of field–line connectivity is to try to understand the relationship between physical quantities in the photosphere at the footpoints of magnetic field lines and the heating process in the corona on the same field lines. If a particular magnetic quantity, such as shear, plays a role in coronal heating then one expects the coronal extension of field lines passing through peaks in this quantity will show the highest coronal temperatures. This idea can be used to test candidate coronal heating mechanisms. We demonstrate these ideas using the combination of high–resolution VLA observations of a complex active region together with state–of–the–art nonlinear force–free field modeling.

**Key words:** Sun: corona — Sun: magnetic fields — Sun: radio radiation — Sun: coronal heating

## 1. Introduction

The determination of magnetic field and temperature of the solar corona is a goal being pursued by a number of complementary techniques. The ability to measure these quantities is widely regarded as an important stepping stone in the path to understanding many of the major unsolved problems of solar physics. Three main techniques contribute to this effort: optical observations of vector magnetic fields in the photosphere and their extrapolation into the corona; EUV/X–ray observations which can reveal the projected paths of magnetic field lines via the density contrast between neighboring bundles of field lines; and radio observations which are sensitive to both the strength and direction of the coronal magnetic field. The three techniques each have their own advantages and disadvantages, and we are presently still very much in the phase of learning how best to use them (e.g., McClymont, Jiao & Mikić 1997; Bastian, Gary, & White 1998). It is clear that the strengths of each technique will have to be combined with those of the others in order to make progress. In particular, the success of extrapolation of photospheric field measurements into the corona needs to be tested against coronal observations. One such test is the comparison of field line trajectories predicted by the field extrapolations with coronal X–ray images which delineate that subset of field lines which carry high densities (e.g., Jiao, McClymont, & Mikić 1997, Golub 1996).

Field–line structure is not as apparent in microwave images as in soft X–rays because the latter show primarily density contrast whereas radio data in active regions, (emission tends to be optically thick) show primarily temperature contrast. Thus radio images are generally not suitable for tracing individual field lines. Instead, comparison

is usually made with magnetic field strength, to which microwave emission has unique sensitivity (see, for more comprehensive references, White & Kundu 1997). In the CoMStOC studies (Schmelz et al. 1994, 1992, Brosius et al. 1992), for instance, the relevant harmonic is evaluated using plasma parameters derived from soft X-ray observations, and the harmonic along with the observing frequency are used in the gyroresonant condition (Zheleznyakov 1962) to derive a coronal field strength. The results were then compared with predictions of potential-field (PF) extrapolations of photospheric magnetic fields; in regions where the comparison failed the fields were argued to be non–potential. Other studies (Schmahl et al. 1982; Alissandrakis & Kundu 1984) have used a linear force-free field (FFF) extrapolation (i.e. fields obeying $\mathbf{J} = \alpha\mathbf{B}$ with spatially uniform $\alpha$, where $\mathbf{J}$ is current density and $\mathbf{B}$ is magnetic field) was used to supplement the potential field assumption (i.e. $\mathbf{J} = 0$). Nindos et al. (1996) carried out full modeling of radio emissions from linear FFF models to investigate how the observed morphology of radio images and the required coronal field strength constrain the choice of $\alpha$. Chiuderi-Drago, Alissandrakis, and Hagyard (1987) used a pair of dipole magnetic fields, but treated heat transfer along the field lines comprehensively, to successfully reproduce the observed radio morphologies. The results from the latter group of studies indicate that the radio data are sensitive not only to the field strength but also to the orientation of the bundle of magnetic field lines.

As the techniques that measure the photospheric fields and reconstruct the coronal fields from them grow more sophisticated (e.g., McClymont, Jiao, & Mikić 1997, Mikić & McClymont 1994), we need a more powerful means to relate active region radio emission to such magnetic field models. In this paper, we propose to use field line connectivity between the corona and the photosphere as a main criterion in comparison. Due to rapid field–aligned transport of physical quantities in solar corona, there are strong theoretical reasons for expecting that the temperatures at points in the corona connected by the same field line should be well correlated (Rosner, Tucker, & Vaiana 1978, Craig, McClymont, & Underwood 1978, Kankelborg et al. 1996). As long as the observed radiations are dominated by optically thick gyroresonance emission, the radio images we obtain at two different frequencies represent true local coronal electron temperatures on thin isogauss surfaces in the corona. This suggests two things: first, we should see a good correlation in temperatures observed at two different frequencies at points connected by common field line if the field line model accurately represents the connectivity and if we can determine the appropriate harmonic correctly. Conversely, whether a given field extrapolation model can predict such a correlation or not is a measure of the success of the extrapolation technique. Secondly, if we compare the coronal temperature sensed by radio observation with magnetic quantities observed in the photosphere (such as $\mathbf{J}$, $\alpha$, or $\mathbf{B}$) at the points connected by common field lines, we may learn which quantity in the photosphere best correlates with the temperature of its coronal counterpart. Such a correlation can be used to test theoretical ideas on coronal heating mechanisms, in view of studies which consider coronal heating as a coronal response to photospheric perturbations (Parker 1972, 1983, Mikić, Schnack, & Van Hoven 1988, Longcope & Strauss 1994, Gomez, DeLuca, & McClymont 1995). Here we explore these ideas using radio and magnetic data for AR 6615, for which we have both excellent radio observations at 4.9 GHz (resolution $8''$) and 8.4 GHz (resolution $5''$) made using the VLA on 1991 May 7 and a state-of-the-art nonlinear force-free-field (FFF) extrapolation of the photospheric vector magnetic field performed using the evolutionary technique (see, for details, Lee et al. 1997, Lee et al. 1998ab).

## 2. Test of Coronal Magnetic Field Extrapolations

The top panel of Figure 1 shows, for the purposes of illustration, the observed intensity distributions at 4.9 GHz and 8.4 GHz on two hypothetical, simplified emission layers (simplified in the sense that the true isogauss surfaces are not flat as represented in this figure). Here $(x, y)$ is the sky plane and $z$ is the line of sight. According to the magnetogram (from the polarimeter of Mees Solar Observatory) the magnetic field is nearly potential in region A and highly sheared in region B. It is our goal here to compare the field–line connectivity in the PF and FFF models for regions A and B separately using the brightness temperature measurements from the radio data. If the test is valid and if the FFF extrapolation is successful, then we expect that it should be superior to the PF model in region B.

We start at a point in one of the emission layers (here the 4.9 GHz emission layer) and trace the field line passing through this point until it hits the other emission layer (the 8.4 GHz emission layer), if it does so (like field lines numbered 1–3); if it does not (like field line 4), we ignore it. In order to locate the appropriate layers within the extrapolation, however, we need to know the relevant harmonic, i.e., the highest optically–thick harmonic. We have no way to estimate the harmonic but to use the theoretical gyroresonant opacity (Zlotnik, 1968). Having a field extrapolation model, it is easy to calculate the required magnetic quantities such as magnetic field inclination angle and magnetic scale height at all harmonic layers (e.g., Fig. 4 of Lee et al. 1998a). For the electron temperature on the relevant harmonic layers, we use the observed radio temperatures as trial values. Densities are then derived

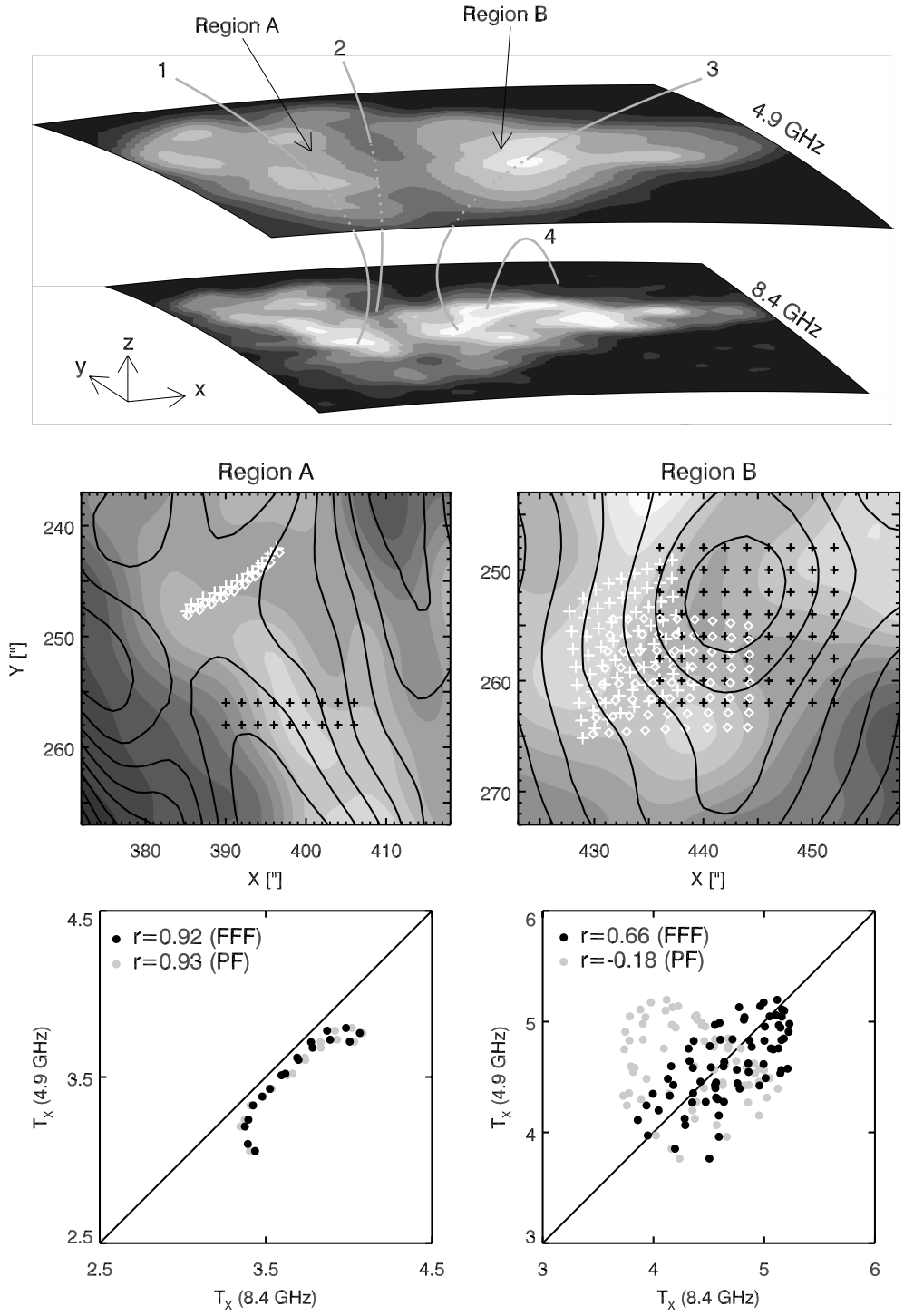


Fig. 1.. The figure in the top panel illustrates the proposed method. The two surfaces shown are hypothetical emission layers for 4.9 and 8.4 GHz, respectively, and the greyscale images on the surfaces are the actual observed X mode microwave images of AR 6615. The coordinates $(x, y)$ form the sky plane, while $z$ is the line of sight. The middle panels shows contours of the X-mode 4.9 GHz image in region A (left) and region B (right) plotted on a greyscale presentation of the 8.4 GHz data, together with a grid of points on each layer representing the intersections of field lines with each layer. Black plus symbols show the intersections of the field lines with the 4.9 GHz layer: these are the starting points for both the PF and FFF extrapolations. Their intersections with the 8.4 GHz layer are represented (in projection onto the sky plane) by white plus symbols for the PF field lines and by white diamonds for the FFF field lines. The bottom panels are the scatter plots of 4.9 GHz brightness temperature versus that at 8.4 GHz at points connected by the potential field lines (grey dots), and by nonlinear force–free field lines (black dots), respectively. $r$ is the linear correlation coefficient.

per field line using temperature and lengths of the field lines passing through the harmonic layers in the well–known scaling law for quasistatic loops of Rosner, Tucker, and Vaiana (1978). All these quantities evaluated on the harmonic layers of concern are used to calculate theoretical gyroresonant opacities at the two observing frequencies. Due to unusually high temperature ($\sim 6\times10^6$ K) for this active region, it is found that two hottest parts of the active region can be optically thick up to the fourth harmonic in the X mode. We have no independent method to determine the appropriate harmonic, but note that if our determination is incorrect we expect that the temperature correlation will not be observed.

The assumption $n = 4$ means that the 4.9 and 8.4 GHz emission layers are the isogauss surfaces in the corona at 430 G and 750 G, respectively. We thus determine the positions of 430 G and 750 G surfaces in each magnetic field model and perform field line tracing from the 430 G isogauss surface to the 750 G isogauss surface to determine the intersections on the 750 G surface. The two middle panels of Figure 1 show the positions determined in this way in regions A and B, respectively. Here the starting points on the 4.9 GHz surface are shown as black crosses and form a regular rectangular grid of uniform spacing in projection, while the white plus and diamond symbols are those connected by potential field lines and nonlinear force–free field lines, respectively. Ideally, this comparison has to be made over an area as wide as possible in which a common harmonic is considered adequate. In region A, however, we confine the comparison to a small area because most field lines passing through the brighter part of the 8.4 GHz emission do not reach the height of the 4.9 GHz emission layer as exemplified in the top panel of Figure 1.

The bottom panels show the corresponding scatter plot of brightness temperature at 4.9 GHz vs. that at 8.4 GHz for the connected points along with the linear correlation, $r$, at X mode in particular. In region A (the bottom left panel of Fig. 1), the PF and the FFF extrapolation should produce a similarly good result if the field there is indeed potential–like. The fact that resulting temperature correlation is excellent confirms the present approach. In region B (the bottom right panel of Fig. 1), the presence of strong currents affects the magnetic structure in the corona and points in the two layers connected by field lines in the FFF model are very different from those in the PF model; while the connection in the PF model results in a negative correlation ($r = -0.18$), the field lines from the FFF model result in a good correlation ($r = 0.66$) between the two layers. This proves that the FFF predicts the correct behavior for field lines in this region whereas the PF model does not.

## 3. Study of Coronal Heating above Active Regions

Many observational studies of coronal heating compare bright X-ray or EUV emissions with magnetic quantities in the underlying photosphere in order to determine the properties of the heating mechanism (e.g., Metcalf et al. 1994, Kankelborg et al. 1996, Fisher et al. 1998). We can equally well compare a coronal property connected to the photosphere by a magnetic field line as we can compare it with elsewhere in the corona. This leads to a study in which we compare the predictions of empirical models for coronal heating with measured coronal temperatures on field lines in the framework of the so-called Field–Line–Structured Temperature (FLST) model (Lee et al. 1998a). Figure 2 shows some of the results.

In the initial models we ignore any dependence of temperature on position along the loop and assume instead that the temperature is uniform along a given field line and proportional to one of the quantities, $\{B, |\alpha|, J\}$ at a footpoint. The results of radio images predicted from these temperature models at 8.4 GHz are shown in Figures 2(a) to 2(c), respectively. It appears that the third model hypothesis ($T_e \sim J$) leads to a better result in that it reproduces the radio peaks in both regions A and B whereas the other two hypotheses yields results good in either region A or region B but not both (cf. Jiao, McClymont, and Mikić 1997). However, the overall agreement between models and observation is not satisfactory in any of the models.

We thus consider alternative FLST models employing $T_e \sim J$ in which temperature on a loop varies as a function of arc length from the loop-top. Theoretically a coronal loop in quasi-static equilibrium should have highest electron temperature at its top and the temperature elsewhere should decrease with arc length, i.e., the distance along the field line from the loop top (Rosner, Tucker, and Vaiana, 1978; Craig, McClymont, and Underwood, 1978). We note that in Rosner, Tucker, and Vaiana's (1978) model, the temperature variation with arc length $l$ is well approximated by a simple power law: $T_e(l) \sim l^{1/2}$ (their Fig. 11). To incorporate this physics into the present model we use, instead of a uniform temperature model, the form $T_e(l) = T_{\rm base} + T_e^{\rm top}(l/L)^{1/2}$ where $l$ is the arc length measured from the footpoint to the position of gyroresonant point in the loop and $L$ is the half arc length of the loop; $T_e^{\rm top}$ is still determined by the current density, $J$, at the footpoint. Figure 2(d) shows a model radio image obtained using such a temperature model. Finally we allow for the possibility that the actual emission layer could be located higher than we modeled if the photospheric magnetic field measurement were off by a certain amount or if the model fields were insufficiently relaxed to the force-free state. For this purpose we multiply the present magnetic field model by

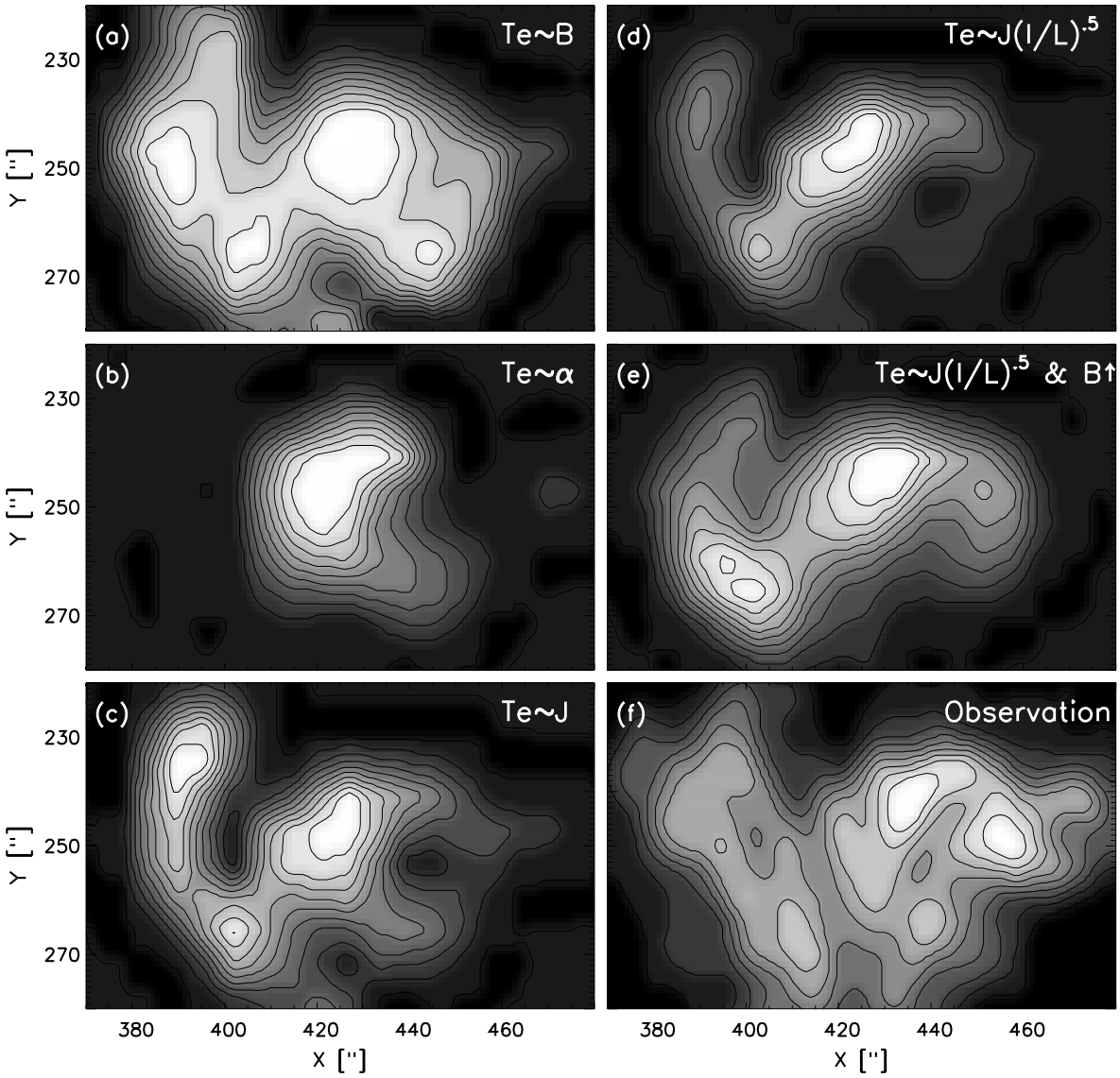


Fig. 2.. Model radio intensities vs. observed intensity at 8.4 GHz. The key assumption made in each model is written in the upper-right corner in (a)–(e). The observed radio intensity at 8.4 GHz is shown in (f) for comparison.

a constant factor of 1.3 and redo the above calculation. The result is shown in Figure 2(e), which is remarkably similar to the observation (Fig. 2(f)).

Why does the hypothesis that temperature of a loop is proportional to the current density entering the loop work here? Although we cannot provide a firm interpretation of this result, our speculation at a very superficial level is as follows. By analogy with Jiao, McClymont, and Mikić's (1997) interpretation, we also consider that the efficiency of the interaction between the magnetic fields and turbulence influences heating in the corona and thus the temperature on each loop (cf. Gomez et al. 1995). That efficiency may well depend on the level of turbulence on a field line as well as the field strength. Thus, if the turbulence inside the active region is not evenly distributed in space, but rather is enhanced in some local regions, it is likely that $\alpha$ in those regions tends to be high. Then it would certainly be the case that $J$ rather than $B$ is a better indicator of the coupling between the magnetic fields and turbulence, so that the coronal loop temperature shows a correlation with $J$ in the photosphere. In this sense, our result implies a connection between photospheric magnetic fields, turbulence, and coronal heating as in Parker's theory for coronal heating in active regions (Parker, 1972, 1983).

## 4. Conclusion

Inferring 3D structure is always a difficult task in any astronomical observation which is made with a 2D projection. The reason why we nevertheless expect 2D radio images in particular can be used to probe the 3D coronal structure is that this is a resonant phenomenon and represents the true electron temperature on a thin slice of the corona and the third dimension is provided by the frequency. In addition to this, we rely on the theoretical expectation that due to rapid transport of physical quantities in the corona along field lines, coronal temperature should be structured along field lines and further there is a relationship between temperature and density per loop for quasistatic equilibrium (Rosner, Tucker, & Vaiana 1978, Craig, McClymont, & Underwood 1978). In our results, the assumption that the coronal temperature would be nearly uniform on a given field line was adequate for testing between different extrapolation models, because all we needed was to see which yields the better temperature correlation whatever the actual dependence of temperature on position in the loop is. Note also that we limited the test to regions where the temperatures are high and magnetic fields are strong enough to be sure of the relevant harmonic and the dominant radiation mechanism. In order to obtain agreement between the model and observation over the whole active region, however, we needed minor corrections to allow variation of temperature along a loop at low heights consistent with the theory of quasistatic equilibrium of coronal loops (Rosner, Tucker, & Vaiana 1978). In the future, coronal field extrapolation might be able to predict not only magnetic fields but to determine the temperature and density on each field line as well, by treating fully thermodynamics along individual field lines (in fact, similar to Chiuderi-Drago et al. 1987). The coronal heating function is not determined by such an extrapolation but remains to be determined, hopefully with the help of constraints provided by comparison with radio data.

This work has been supported by NSF grant ATM-96-12738 and NASA grant NAG-W-1541. JL is supported by NASA grant NAG5-6381. ZM has been supported by NASA contract NASW-4728 and NSF grant ATM-9320575.

## References

Alissandrakis C.E., Kundu M.R. 1984, A&A 139, 271
Bastian, T. S., Gary, D. E., White, S. M. 1998, in Synoptic Solar Physics, eds. K. S. Balasubramaniam, J. W. Harvey and D. M. Rabin, Astron. Soc. Pacific (San Francisco), p.
Brosius, J. W., Wilson, R. F., Holman, G. D., Schmelz, J. T. 1992, ApJ, 386, 347
Chiuderi-Drago, F., Alissandrakis, C., Hagyard, M. 1987, SolPhys, 112, 89
Craig, I. J. D., McClymont, A. N., Underwood, J. H. 1978, A&A, 70, 1
Fisher, G.H., Longcope, D.W., Metcalf, T.R., Pevtsov, A.A. 1998, ApJ, 508, in press
Golub, L. 1996, Ap&SS, 237, 33.
Gomez, D. O., DeLuca, E. E., McClymont, A. N. 1995, ApJ, 448, 954
Jiao, L., McClymont, A. N., Mikić, Z. 1997, SolPhys, 174, 311
Kankelborg, C. C., Walker A. B. C., Hoover, R. B., Barbee, T. R., Jr. 1996, ApJ, 466, 529
Lee, J., McClymont, A. N., Mikić, Z., White, S. M., Kundu, M. R. 1998a, ApJ, 501, 853
Lee, J., White, S. M., Kundu, M. R., Mikić, Z., McClymont, A. N. 1998b, SolPhys, 180, 193
Lee, J., White, S. M., Gopalswamy, N., Kundu, M. R. 1997, SolPhys, 174, 175
Longcope, D. W., Strauss, H. R. 1994, ApJ, 426, 742
McClymont, A. N., Jiao, L., Mikić, Z. 1997, SolPhys, 174, 191
Metcalf, T. R., Canfield, R. C., Hudson, H. S., Mickey, D. L., Wulser, J.-P., Martens, P. C. H., Tsuneta, S. 1994, ApJ, 428, 860
Mikić, Z., McClymont, A. N. 1994, in *Solar Active region Evolution: Comparing Models with Observations*, ed. K. S. Balasubramaniam & G. Simon, A.S.P. Conf. Series, 68, 225
Mikić, Z., Schnack, D. D., Van Hoven, G. 1988, ApJ, 338, 1148
Nindos, A., Alissandrakis, C. E., Gelfreikh, G. B., Kundu, M. R., Korzhavin, A. N., Bogod, V. M. 1996, SolPhys, 166, 55
Parker, E. N. 1972, ApJ, 174, 499.
Parker, E. N. 1983, ApJ, 264, 642.
Rosner, R., Tucker, W. H., Vaiana, G. S. 1978, ApJ, 220, 643
Schmahl, E. J., Kundu, M. R., Strong, K. T., Bentley, R. D., Smith, J. B., Krall, J. R. 1982, SolPhys, 80, 233
Schmelz, J. T., Holman, G. D., Brosius, J. W., Gonzalez, R. D. 1992, ApJ, 399, 733
Schmelz, J. T., Holman, G. D., Brosius, J. W., Wilson, R. F. 1994, ApJ, 434, 786
White, S. M., Kundu, M. R. 1997, SolPhys, 174, 31
Zheleznyakov, V. V. 1962, Soviet Astron, 6, 3
Zlotnik, E. Ya. 1968, Soviet Astron, 12, 245